ELSEVIER

Cardiovascular Research 45 (2000) 941–951

Cardiovascular Research

www.elsevier.com/locate/cardiores
www.elsevier.nl/locate/cardiores

Human connexin40 gap junction channels are modulated by cAMP

Harold V.M. van Rijen*, Toon A.B. van Veen, Monique M.P. Hermans, Habo J. Jongsma

Department of Medical Physiology and Sports Medicine, Faculty of Medicine, Utrecht University, PO Box 80043, 3508 TA Utrecht, The Netherlands

Received 26 April 1999; accepted 13 October 1999

Abstract

Objective: Gap junction channels provide for direct electrical coupling between cells, and play an important role in homeostasis and electrical coupling. One of the proteins that form gap junctions, Connexin40 (Cx40), shows restricted expression in the body, and is found in blood vessels and in the atrium and conduction system of the heart. We have investigated whether gap junction channels formed of Cx40 are modulated by protein-kinase-A-mediated phosphorylation. **Methods:** A communication-deficient human hepatoma cell line (SKHep1) was stably transfected with human Cx40 cDNA and the properties of Cx40 gap junctions channels and their modulation by cAMP were analyzed using immunocytochemistry, Western blotting, dual patch clamp, and dye coupling. **Results:** Administration of 1 mM 8-Br-cAMP resulted in a mobility shift of Cx40 protein on western blot and increased macroscopic gap junctional conductance between cell pairs by 46.2±12.0% (mean±S.E.M., $n=8$). Under control conditions, single channel experiments revealed three single channel conductances around 30, 80 and 120 pS. When cAMP was added, channel conductances of 46 and 120 pS were observed. In monolayers, cAMP also increased the permeability of Cx40 gap junction channels for Lucifer Yellow by 58%. **Conclusions:** Macroscopic conductance and permeability of Cx40 gap junctions is strongly increased by cAMP and may play a role in the regulation of intercellular communication in the heart and vasculature.

Keywords: Adrenergic (ant)agonists; Gap junctions

This article is referred to in the Editorial by J.E. Saffitz and K.A. Yamada (pages 807–809) in this issue.

1. Introduction

Gap junctions are agglomerates of intercellular channels, forming a direct pathway between the cytoplasms of neighbouring cells. These channels are formed by head to head alignment of two hemichannels, called connexons, each composed of six connexin (Cx) molecules. Up to now, 13 mammalian connexins have been cloned and named after their theoretical molecular mass. The putative structure of connexins in this gene family is similar and although the amino acid sequence of the transmembrane and extracellular regions is largely conserved, that of the intracellular domains is very divergent. Gap junctional properties and their regulation in a certain tissue are mainly determined by the connexin types locally expressed (for recent review see [1]).

Cx40, a member of the connexin family shows a restricted expression pattern in mammals and was found to be expressed in the atrium and conduction system of the heart [2–8], lung [9], vascular smooth muscle cells [10–12], and vascular endothelium [3,4,12–16].

The electrical conductance of single Cx40 gap junction channels was the subject of previous investigations and amounted to values between 120 and 200 pS, dependent on the experimental conditions [14,17–19]. Furthermore, the Cx40 protein contains putative phosphorylation sites for PKC, PKA, and PKG [9,11,20–22]. Exposure of cells expressing mouse Cx40 to cAMP and TPA, thereby activating protein kinase A (PKA) and protein kinase C (PKC), respectively, both increased the phosphorylation of Cx40 [14]. The biophysical significance of Cx40-phosphorylation is not clear as yet.

*Corresponding author. Tel.: +31-30-253-8900; fax: +31-30-253-9036.

E-mail address: h.v.m.vanrijen@med.uu.nl (H.V.M. van Rijen)

Time for primary review 18 days.

0008-6363/00/$ – see front matter
PII: S0008-6363(99)00373-9

However, because of its restricted distribution, the regulation of Cx40 gap junction channels is of interest. Especially in the heart, where Cx40 is regionally expressed in the atria and conduction system, short term modulation of the conductance of Cx40 gap junction channels might alter the propagation of the cardiac impulse.

In order to study the electrical properties and permeability of Cx40 gap junction channels in isolation and their modulation by cAMP-mediated phosphorylation, we have stably transfected cells of a communication deficient human hepatoma cell line (SKHepl) with human Cx40 DNA. The effect of cAMP on phosphorylation and the electrical conductance of gap junction channels formed between these cells was studied using the dual voltage clamp technique, whereas the effect of cAMP on the permeability of the Cx40 gap junction channels for larger molecules was assessed by diffusion of Lucifer Yellow (dye coupling).

2. Methods

2.1. Cloning of connexin40 (Cx40) from human umbilical cord venous cells

Human umbilical cords were obtained with informed consent, according to the rules of the medical ethical committee of the Utrecht academic hospital. From the umbilical cord vein, endothelial cells were isolated as described previously [15]. Human Cx40 was PCR amplified from genomic DNA of cultured human umbilical vein endothelial cells (HUVEC), with primers corresponding to the amino-(P21s: CCGGAATTCATGGGCGATTGGAGCT) and carboxytermini (P22a: CCAAGATCTGGG TCACACTGATAGG) of human Cx40 as published by Kanter et al. [22]. In this way the complete open reading frame of Cx40, including the start and stopcodons, was amplified. The primers P21s and P22a contained an extra *Eco*RI and *Bgl*II restriction site, respectively, to facilitate cloning in the eukaryotic expression vector pSG5 (Stratagene). The PCR reaction was performed in a final volume of 25 μl containing 1 μM of each primer, 2.5 μg genomic DNA, 0.2 mM of each deoxyribonucleotide (Pharmacia Biotech), 1.5 mM $MgCl_2$, 50 mM KCl, 10 mM Tris–HCl (pH 9.0) and 1 U Taq-polymerase (Pharmacia Biotech). PCR was performed as follows: initial heating for 2 min at 94°C; 5 cycles (94°C, 30 s; 50°C, 1 min; 72°C, 1 min); 30 cycles (94°C, 30 s; 59°C, 1 min; 72°C, 1 min); final extension 7 min at 72°C. The obtained PCR fragment was phenol purified, precipitated and digested with 10 U *Bgl*II and 10 U *Eco*RI for 3 h at 37°C. The digested DNA was separated on an agarose gel. The Cx40 fragment was cut out, purified via GeneClean (Bio 101) and cloned in pSG5 in the *Eco*RI and *Bgl*II sites. The construct used for expression experiments was checked by double-strand DNA sequencing using the T7 sequencing kit (Pharmacia Biotech).

2.2. Expression in SKHep1 cells

SKHepl cells (human hepatoma) were obtained from the American Type Culture Collection (Rockville, MD) and cultured in Dulbecco's modification of Eagle's medium supplemented with fetal calf serum (10%) and antibiotics under 5% CO_2 at 37°C. Stably transfected cells expressing human Cx40 were generated as described before [23]. Colonies were screened for gap junctional coupling by micro-injection of Lucifer Yellow (4% in 150 mM LiCl, buffered to pH 7.2 with 10 mM HEPES). After a 2 min diffusion time, cell coupling was determined by counting the number of fluorescent cells under an inverted microscope (Nikon Diaphot). Colonies that allowed transport of the dye between the cells were further analyzed for Cx40 expression using standard RT-PCR techniques on total cellular RNA extracts.

2.3. Immunocytochemistry

SKHep1/hCx40 cells were grown to subconfluency on glass coverslips, rinsed in phosphate buffered saline (PBS) and subsequently fixed in methanol (−20°C) for 2 min. They were stored in PBS at 4°C. Fixed cells were permeabilized with 0.2% Triton X-100 in PBS for 1 h. Subsequently, nonspecific binding of primary antibody was blocked with 2% bovine serum albumin (BSA) for 30 min. Primary antibody incubations were performed overnight, with antibodies raised against Cx40 (Alpha Diagnostics, 0.5 μg/ml PBS/10% Normal Goat Serum [NGS]) and Cx45 (Alpha Diagnostics, 5 μg/ml PBS/10% NGS). All incubation steps were performed at room temperature (20–23°C), and in between all incubation steps, cells were thoroughly washed with PBS. Next day, cells were preincubated with 2% BSA in PBS. Immunolabeling was carried out using fluorescein isothiocyanate (FITC-conjugated secondary antibodies (Jackson Immunostaining) against rabbit IgG. Coverslips were mounted in Vectashield (Vector Laboratories) and examined with a Nikon Optiphot-2 light microscope equipped for epifluorescence.

2.4. SDS–PAGE and Western Blot

Cells destined for protein isolation were grown to subconfluency in 10-cm diameter Costar tissue culture disks. Prior to treatment, the cells were washed extensively with PBS and normal culture medium was replaced for 2 h by serum-free medium. In order to activate PKA, 1 mM 8-Br-cAMP was added to the cultures. After 10 min, incubations were stopped by washing the cells with PBS. Subsequently, cells were collected in lysis buffer (400 μl/10 cm dish; 50 mM Tris–HCl pH 7.4, 150 mM NaCl, 0.5% Nonidet-P40, 0.5% sodium deoxycholaat, 0.1%

sodium dodecyl sulfate (SDS), 2 mM phenylmethylsulfonyl fluoride (PMSF), protease-inhibitor-cocktail) and sonicated on ice (3×10 s, 60 W, Branson Sonic Power). Cellular debris was concentrated by centrifugation (5 min, 14 000 rpm) and total cellular protein in the supernatant was determined using the Lowry protein assay [24].

Aliquots were diluted with 4× Laemmli buffer and boiled for 5 min. Equal amounts (50 μg per lane) of each sample were separated overnight (80 V) on 10% SDS–polyacrylamide gels [25], (18×24 cm) and electrophoretically transferred (4°C, 3 h, 350 mA) to nitrocellulose membrane (0.45 μm, Biorad). Protein transfer was assessed by Ponceau S staining. Prior to primary antibody incubation, the nitrocellulose membrane was blocked with 5% dried milk powder (1 h, RT, in 0.1% Tween20/PBS). Blots were incubated overnight at 4°C with primary antibodies raised against mouse Cx40 (Alpha Diagnostics, 4 pg/ml in 0.1% BSA/0.1% Tween20/PBS) or mouse Cx45 (kind gift from Dr. T.H. Steinberg, crude serum 1:2000 in 0.1% BSA/0.1% Tween20/PBS). Next morning, the membrane was washed (3×5 min, 0.1% Tween20/PBS), incubated with horseraddish-peroxidase-conjugated second antibody (1 h, 4°C, 0.1% BSA/0.1% Tween20/PBS) and washed again (6×5 min, 0.1% Tween20/PBS). Signals were visualized by 1 min development in Enhanced Chemo Luminiscence reagent (ECL, Amersham) and exposure to XB-1 film (Kodak).

2.5. Dye coupling experiments

Before starting the experiment, the culture medium was replaced by a protein-free control solution containing (in mM): 94.1 NaCl, 5.4 CsCl, 10.7 Na_2HPO_4, 23.8 $NaHCO_3$, 0.4 $CaCl_2$, 0.4 $MgSO_4$, 11.1 glucose, 25.0 *N*-2-hydroxyethyl-piperazine-*N′*-2-ethanesulfonic acid (HEPES), pH 7.4 (adjusted with NaOH). All experiments were performed at room temperature (20–23°C). Microelectrodes (tip diameter <1 μm) were pulled from 1.0-mm borosilicate capillaries and backfilled with 4% Lucifer Yellow CH (LY) in 150 mM LiCl. Petri dishes containing monolayers of transfected cells were placed on the stage of an inverted microscope (Nikon Diaphot TMD), and observed at a total magnification of 400× using phase-contrast optics and epifluorescence. The microelectrode was inserted into a cell using a hydraulic micromanipulator (M0203, Narishige). Subsequently, the dye was allowed to diffuse out of the pipette into the impaled cell and adjacent cells for 5 min before the electrode was retracted. This resulted in hardly any leakage of LY from the cells, indicating fast membrane sealing. Then the number of stained cells (including the impaled one) was counted.

2.6. Electrophysiological measurements

Patch pipettes were pulled with a vertical electrode puller (Narishige PB-7) from 1-mm borosilicate capillaries with inner filament. Electrode tips were heat polished and the pipettes were backfilled with 0.22 μm filtered solution containing (in mM): 130 K-gluconate, 10 KCl, 10 $MgCl_2$, 0.6 $CaCl_2$, 10 ethylene glycol-bis(β-aminoethyl ether)-*N,N,N′,N′*-tetraacetic acid (EGTA) ([free Ca^{2+}]=23.5 nM [26]), 5 Na_2ATP, 10 HEPES, pH 7.2 (adjusted with KOH). Typical electrode resistance was 5 MΩ as measured in the control solution (for composition see dye coupling experiments).

Cultured cells in petri dishes were placed on the stage of an inverted microscope (Nikon Diaphot TMD) equipped with Hoffman modulation contrast optics and observed at a total magnification of 400×. Electrodes were lowered onto cell pairs using hydraulic micromanipulators (M0203, Narishige). After formation of gigaohm seals, the membrane patch under the electrode was broken by gentle suction to obtain the whole cell configuration.

Macroscopic and microscopic gap junctional currents were measured using the dual voltage clamp technique [27,28] with two patch clamp amplifiers (Dagan 8900). Command potentials and elicited currents were digitized at 1 kHz using a custom computer program (Scope, kindly provided by J. Zegers, Department of Physiology, University of Amsterdam) running on a Macintosh microcomputer (Apple), equipped with a 12-bit AD-board (National Instruments).

Initially, both cells of a pair were voltage-clamped at 0 mV, close to the membrane potential. Next, the holding potential of one of the cells was changed stepwise to 50 mV, generating a voltage difference across the gap junction (V_j). This V_j evokes a current in each cell: the sum of the membrane and the junctional current in the stepped cell and the junctional current in the non-stepped cell. Gap junctional conductance (g_j) was calculated by dividing the current in the non-stepped cell by V_j, and corrected for series resistance as explained below.

To resolve single gap junction channel events, 2 mM halothane was added to the control solution [29,30].

2.7. Phosphorylating conditions

For each experiment a fresh solution containing 1 mM of the membrane permeant nucleotide 8-bromo-cAMP (8Br-cAMP, Sigma) dissolved in control solution was prepared. In whole cell experiments measuring macroscopic conductance, the superfusion was switched from control to 8Br-cAMP solution after conductance had reached steady state. The specificity of 8Br-cAMP was tested in separate experiments by adding a specific protein kinase A antagonist, Rp-adenosine-3′, 5′,-cyclic phosphorothioate (Rp-cAMPS, Biolog) to the internal pipette solution in a final concentration of 100 μM. At the beginning of the experiment, when the dual whole cell configuration was reached, Rp-cAMPS was allowed to diffuse into the cell for 5–10 min, before cAMP was added.

For single channel and dye coupling experiments, cells were preincubated for 10 min with salt solution containing 1 mM 8Br-cAMP.

2.8. Data analysis

Macroscopic junctional conductance between cell pairs was determined from digitized whole cell currents, using custom software. Since all cells were well coupled, series resistance (R_s) was measured at the start of each experiment in current clamp, and corrected junctional conductance was obtained numerically from measured junctional currents using:

$$g_j = I_b/(V_a - I_a \cdot R_{s,a} - I_b \cdot R_{s,b}) \quad (1)$$

where V_a, I_a, and $R_{s,a}$ are the voltage step, the current, and series resistance, respectively, in the stepped (cell A), and I_b and $R_{s,b}$ are the current and series resistance, respectively, in the non-stepped cell (cell B). For a detailed discussion on this issue see Ref. [31].

Steps in single channel current were measured from digitized current traces and converted into step amplitude histograms, using custom software (MacDAQ, kindly provided by A.C.G. van Ginneken, Department of Physiology, University of Amsterdam), running on a Macintosh microcomputer (Apple).

Mean single channel conductance (γ_j) was determined by fitting a sum of one to three Gaussian distributions to step amplitude histograms, using KALEIDAGRAPH data analysis and graphics presentation software (version 3.0.1, Adelbeck Software).

2.9. Statistics

Groups of observations were compared using a standard paired (modulation of macroscopic conductance) or unpaired (dye-coupling), two-sided, Student's *t* test. Values of $P<0.05$ were considered significant.

3. Results

3.1. Isolation, sequencing, transfection of hCx40

Cloning and sequencing of Cx40 from HUVEC revealed eight base differences (99.3% homology) in the Cx40 sequence compared to the Cx40 sequence from human heart, reported by Kanter et al. [22] (see Table 1). This resulted in six different amino acids.

The cloned HUVEC Cx40 cDNA was stably transfected in SKHep1 cells and was capable of assembling in functional gap junction channels as judged by the transfer of Lucifer Yellow from the injected cell via gap junctions to neighbouring cells (data not shown). Immunocytochemistry confirmed the expression of Cx40 in transfected cells (Fig. 1A). Apart from some intracellular staining, clear punctate labeling at cell borders was found (arrows), the expected location for Cx40 expression. No labeling for Cx40 was found in non-transfected SKHep1 cells (Fig. 1B). In both transfected (Fig. 1C) and non-transfected (Fig. 1D) SKHepl cells Cx45 staining was found, being somewhat less pronounced in transfected than in untransfected cells.

Table 1
Differences between Cx40 of Kanter et al. [22] (EMBL/Genbank accession number U03486) compared to the HUVEC Cx40 studied here. Nucleotide positions counted from the start codon

Nucleotide position	Kanter et al. [22]	This study	Amino acid difference
54	G	A	
130	A	T	Thr-44→Ser
186	C	G	His-62→Gln
258	T	C	
730	T	C	Tyr-244→His
759		Ins C	Leu-254→Ser Trp-255→Val
769		Del T	Ala-256→Gly
822	T	C	–

Scanning the hCx40 sequence for putative phosphorylation sites resulted in two serine residues that can be phosphorylated by PKA, S_{120} and S_{345} [20,21]. To test whether Cx40 is indeed phosphorylated after exposure to cAMP in our experiments, monolayers of SKHepl/hCx40 cells were preincubated to control or cAMP conditions. Total cellular protein was separated by gel electrophoresis and transferred to nitrocellulose membranes.

Exposure to Cx45 antibodies resulted in an aspecific signal at 65 kD, which was detected in both untransfected HeLa cells (used as negative control) and Cx40 transfected SKHepl cells. SKHepl cells showed one specific band at 46 kD, both under control and cAMP conditions (Fig. 2A). Exposure to cAMP did not alter the amount, nor the mobility of Cx45. When blotted for Cx40 (Fig. 2B), one specific band was detected at 40 kD under control conditions, but interestingly, after preincubation of the cells with cAMP, a second band showed up at 42 kD. This second band probably reflects a mobility shift due to cAMP-mediated phosphorylation of Cx40.

3.2. Macroscopic conductance

Since cAMP was able to phosphorylate hCx40, we determined whether this phosphorylation was able to modify the electrical conductance between pairs of SKHepl/hCx40 cells.

Dual whole cell voltage clamp experiments revealed that transfected cells were electrically well coupled: Steady-state junctional conductance (g_j) was 45 ± 10 nS (mean$\pm$S.E.M., $n=8$). After breaking the membrane patches under the electrodes to get electrical access to the cells, junctional conductance (g_j) was monitored for 2–5 min until it reached a steady state value. Usually there was

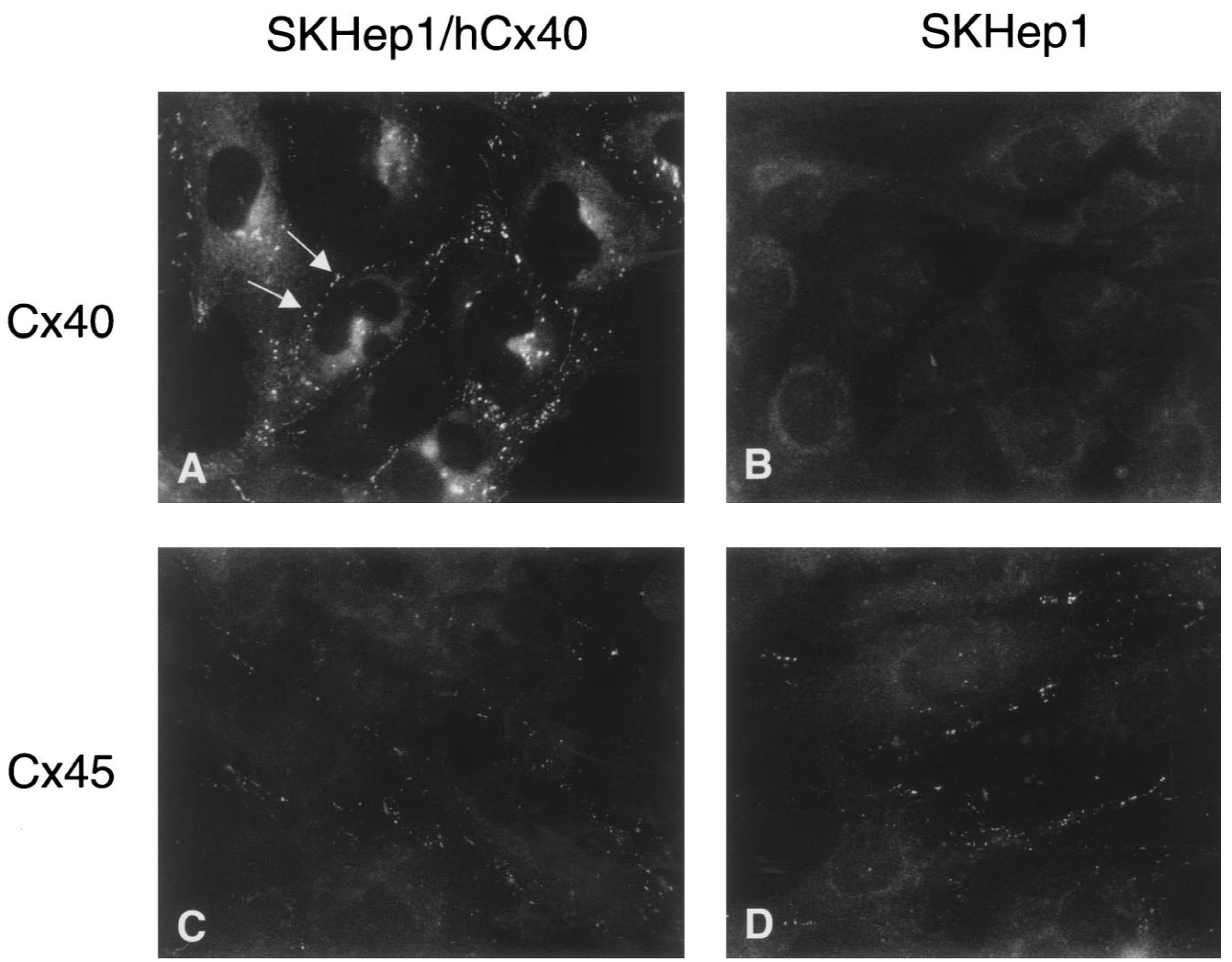

Fig. 1. Immunocytochemical determination of Cx45 and Cx40 expression in hCx40 transfected and untransfected SKHepl cells. Cx40 transfected cells clearly show punctate labeling after incubation with anti Cx40 antibodies (A, arrows), while no staining for Cx40 was found in untransfected cells (B). Both transfected and untransfected cells showed staining for Cx45, although Cx40-transfected cells showed more labeling than untransfected cells (C and D).

an in- or decrease of about 10–20%. Fig. 3A shows a typical experiment. For this cell pair, the initial value of intercellular conductance was 100 nS. After 4 min a steady state g_j of 82 nS was reached. Next, the superfusion was switched from control to the cAMP solution and after a short delay, g_j increased by 70% to a new steady state value of 139 nS. Addition of halothane at the end of each experiment led to complete uncoupling, demonstrating that cell pairs were coupled by gap junction channels only, and not by cytoplasmic bridges. This protocol was applied to another seven cell pairs. On average the g_j of Cx40 gap junction channels increased by 46.2±12.0% (mean±S.E.M., $n=8$) with cAMP in the bath. The increase of the macroscopic conductance of Cx40 gap junction channels by cAMP was highly significant ($P<0.01$). To show that cAMP specifically activates PKA, Rp-cAMPS, a competitive inhibitor for cAMP, was added to the pipette solution. 5–10 min after the whole cell configuration was obtained, the superfusion was switched to cAMP. This resulted in a severe supression of the increase in conductance, normally observed with cAMP (Fig. 3B), which indicates that activation of PKA is required for an increase in gap junctional conductance.

3.3. Single channels

Total gap junctional conductance is given by:

$$g_j = n \cdot P_0 \cdot \gamma_j \quad (2)$$

in which n is the number of channels, γ_j the single channel conductance and P_o the single channel open probability. The strong increase of macroscopic conductance by cAMP may be due to an increase in n, P_o, or γ_j or a combination of these. The rapid evolvement of the effect makes a change in n unlikely. Unfortunately, determination of P_o is

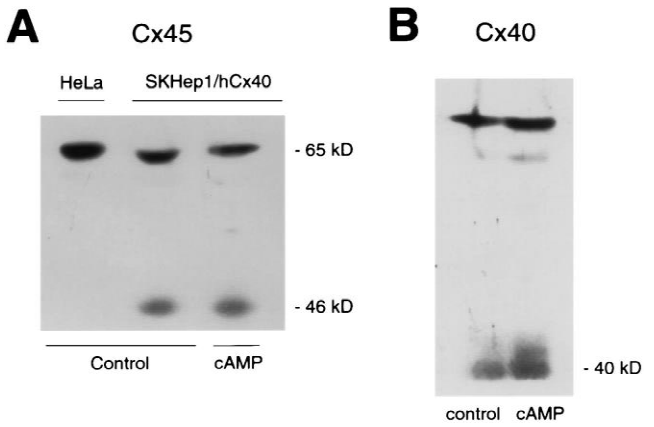

Fig. 2. Western blot analysis of phosphorylation of Cx45 and Cx40 after exposure to cAMP or control conditions in SKHep1/Cx40 transfected cells. (A) Blotting total cell extracts with anti Cx45 antibodies resulted in one aspecific band at 65 kD in both untransfected HeLa cells and Cx40 transfected SKHep1 cells. SKHep1 cells showed one band at 46 kD, both under control and cAMP conditions. No Cx45 specific signal was found in HeLa cells. (B) Similarly, total cell extracts of SKHep1/Cx40 cells were blotted using anti Cx40 antibodies. Under control conditions one specific band is detected at 40 kD. However, after preincubation of the cells with cAMP, a second band shows up at 42 kD. This second band probably reflects a mobility shift due to cAMP-mediated phosphorylation of Cx40.

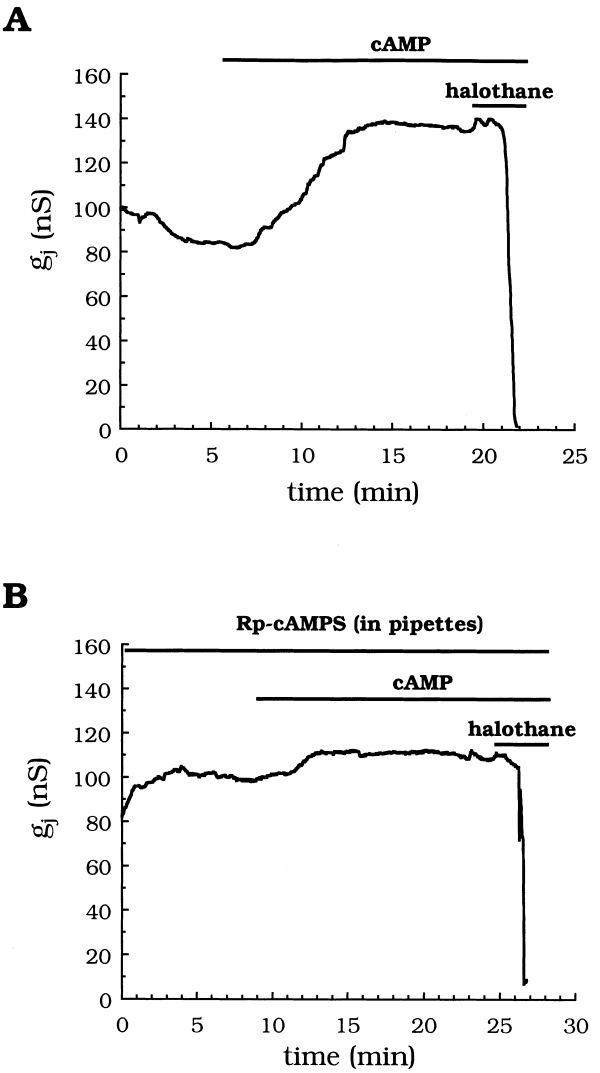

Fig. 3. Effect of cAMP on the macroscopic conductance (g_j), as measured with dual voltage clamp, between SKHep1 cell pairs transfected with human Cx40 DNA. (A) Typical experiment showing the effect of cAMPon junctional conductance. After g_j reached a steady state (82 nS), 1 mM 8-Br-cAMP was added to the bathing solution. After a short delay, there was a strong increase (70%) in conductance between the cells. A new steady state conductance was reached (139 nS) after about 5 min. 2 mM halothane was applied to check whether the electrical coupling between the cells was gap junctional and not (partially) by cytoplasmic bridges. (B) The cAMP-induced increase in conductance was severely supressed in the presence of Rp-cAMPS, a competitive inhibitor for cAMP.

not possible under the experimental conditions, since the gap junctions contain many channels, most of which are closed by halothane. The steps in current are therefore not likely to reflect opening and closing of the same channel. We have therefore investigated the effect of cAMP on γ_j of Cx40 channels.

To be able to observe single channel events at V_j of 50 mV, near zero conductance values were induced by halothane. Three sizes of current transitions were present under control conditions, two of which, of about 120 pS (open circle) and about 80 pS (closed circle) are shown in Fig. 4A. The third current transition represents channels of ~30 pS. After addition of cAMP, only the small conductance of ~30 pS and the large open state of 120 pS were observed (Fig. 4B). All single channel events under control and cAMP conditions are summarized in the frequency histograms of Fig. 4C and D, respectively. Gaussian curve fitting revealed three mean conductances under control conditions, i.e. 30, 82 and 117 pS. After cAMP addition, two mean conductances were found, at 46 and 122 pS. Furthermore, after treatment with cAMP, the channels seemed to spend more time in the open state than under control conditions.

3.4. Dye-coupling

Our results show that cAMP modulated macroscopical and microscopical conductance of gap junctions formed of Cx40. To study whether the permeability of Cx40 gap junction channels for larger molecules, like the fluorescent tracer Lucifer Yellow CH (LY) (molecular weight 443 D [32]) was also affected by cAMP, we performed dye-coupling experiments. Typical experiments are shown in Fig. 5. A single cell in a monolayer was impaled with a LY-filled microelectrode (marked with an asterisk in the phase contrast views (Fig. 5D, E, and F). After 5 min the monolayer was viewed with epifluorescence and the number of stained cells was counted. In these particular experiments eight cells were stained under control conditions (Fig. 5A and D), and 11 cells after exposure to

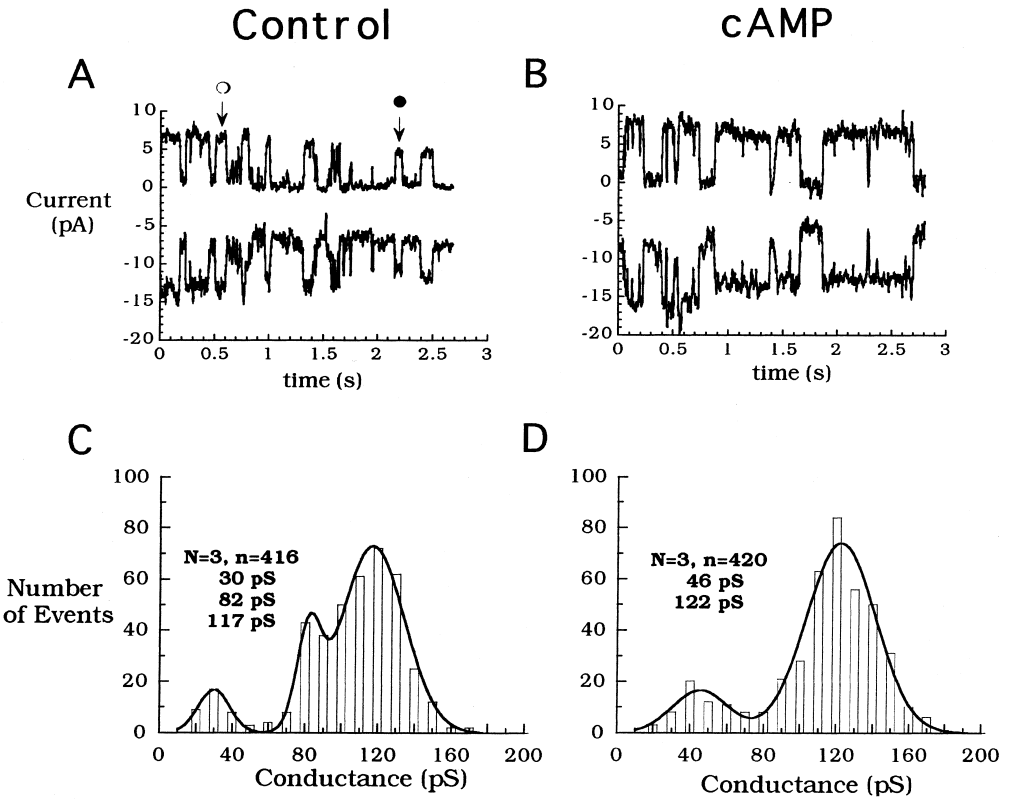

Fig. 4. Effect of cAMP on single gap junction channels in Cx40 transfected cells. In all experiments a driving force of 50 mV was applied. The upper traces of panels A and B represent the current in the non-stepped cell and the lower trace the current in the stepped cell. (A) Single channel currents under control conditions: three current transition sizes are detected, reflecting single channel conductances of about 30, 80 (closed circle) and 120 pS (open circle). (B) Single channel currents after pre-incubation with 1 mM 8Br-cAMP. Only the smallest (~30 PS) and largest (~120 pS) channel conductance were detected. (C) Frequency histogram under control conditions ($N=3$, $n=416$). Gaussian curve fitting revealed three channel sizes: 30, 82, and 117 pS. (D) The frequency histogram under cAMP conditions ($N=3$, $n=420$). The mean conductances from the gaussian fit were 46 and 122 pS.

cAMP (Fig. 5B and E). In the presence of 2 mM halothane only the impaled cell was stained with Lucifer Yellow (Fig. 5C and F).

Fig. 6 summarizes our results for a total of 15 dye experiments under control conditions and another 15 experiments with 8-Br-cAMP added to the bath solution. On average, LY diffused to 8.1±0.4 (mean±S.E.M., $n=15$) cells under control conditions. When cAMP was present, the number of stained cells was increased by 58% to 12.8±0.4 (mean±S.E.M., $n=15$). Means were significantly different ($P<0.0001$) (Fig. 6).

4. Discussion

4.1. Cx40 gene sequence

In the HUVEC-derived Cx40 gene several differences were found as compared to the previously published sequence [22]. Interestingly, two of these differences, i.e., Thr-44→Ser and His-62→Gln were alterations to amino acids found in the Cx40 proteins from rat [11] and mouse [9] at these positions. However, two (unpublished) Cx40 sequences were submitted to Genbank (Lin et al. 1994, accession number L34954, and Haefliger et al. 1999, accession number AF15 1979), which were both identical to our HUVEC Cx40 DNA sequence. Additional Cx40 sequences from at least five other humans were determined in our laboratory, which were all identical to that presented here and published in Genbank (W.A. Groenewegen, pers. comm.). The discrepancy between the Cx40 sequence published by Kanter et al. [22] and those published by our and other groups might reflect a polymorphism. However, the number and locations of putative phosphorylation sites for PKC, PKG, or PKA is identical in all Cx40 sequences, indicating that regulational parts of the protein for those kinases are presumably not affected.

4.2. Macroscopic conductance of Cx40 is increased by cAMP

After exposure to cAMP, the macroscopic conductance between SKHep1 cells transfected with human Cx40 cDNA was increased by 46.2±12.0% (mean±S.E.M., $n=8$). Western blot analysis revealed that this increase in junctional conductance after exposure to cAMP is associated with a mobility shift of the Cx40 protein, reflecting actual phosphorylation of the protein. The fact that the

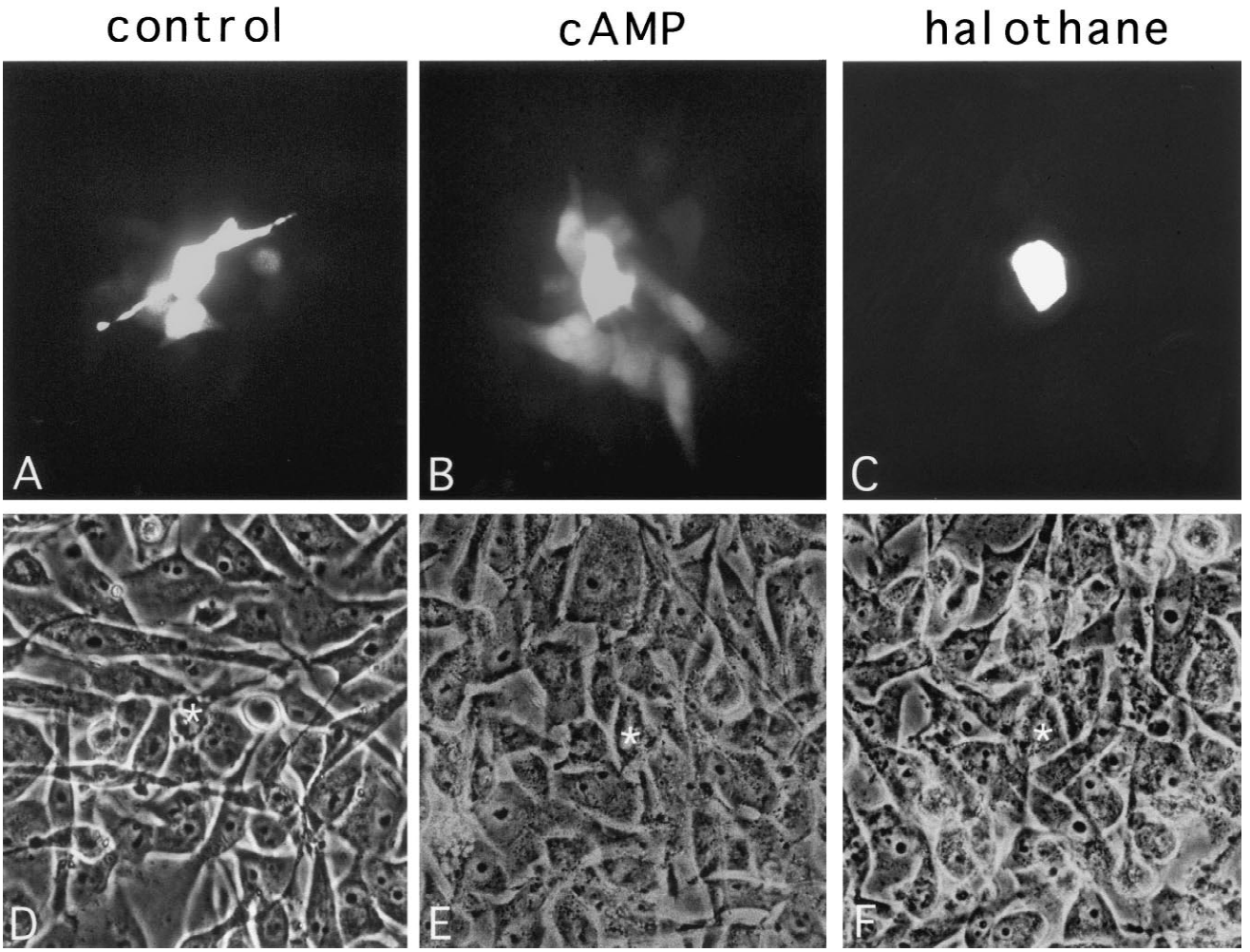

Fig. 5. Dye-coupling in Cx40 transfectants. Microelectrodes filled with the fluorescent dye Lucifer Yellow were inserted into a single cell of a monolayer and the dye was allowed to diffuse from the pipette into the impaled and neighbouring cells for 5 min. (A) control conditions, eight cells stained. (B) Eleven cells stained after exposure to cAMP. (C) 2 mM halothane uncouples the cells: only the impaled cell received LY. (D, E, and F) Phase contrast view of A, B, and C, respectively. The asterisk marks the impaled cell.

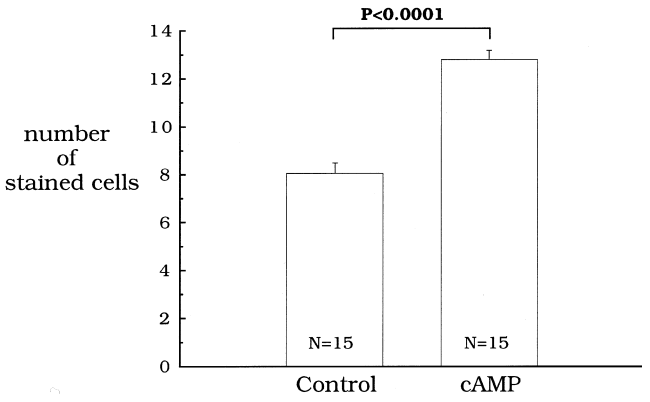

Fig. 6. Statistics of dye-coupling experiments. Under control conditions the dye diffused to 8.1±0.4 cells (mean±S.E.M., $n=15$). When the cells were pre-incubated with 1 mM 8Br-cAMP for 10 min, the number of cells receiving the dye increased by 58% to 12.8±0.4 cells (mean±S.E.M., $n=15$). Means were significantly different ($P\leq 0.0001$).

increase in junctional conductance was blocked after preincubation of the cells with Rp-cAMPS shows that this effect is due to specific activation of PKA and subsequent phosphorylation of the Cx40 protein.

The immunocytochemical experiments revealed that Cx45 is also expressed, though in low amounts, which is in agreement with previous reports [33–35]. Modulation of Cx45 gap junction channels could therefore at least partially account for the observed effect. However, previous measurements on identical cells showed that the electrical conductance of untransfected SKHep1 cells is only 3 nS [35]. Since average conductance between tranfected cells is fifteen times higher, modulation of Cx45 based gap junction channels can only account for the observed effect if their total conductance is increased by 700%, which is highly unlikely. Furthermore, exposure to cAMP did not alter the single channel properties, nor the dye permeability of Cx45 based gap junctions between untransfected SKHep 1 cells [35].

4.3. Single channel characteristics

Under control conditions we found in Cx40 transfected SKHepl cells three single channel sizes close to 30, 80, and 120 pS. Other studies on human Cx40 have shown that when expressed in Jar cells, single channel conductances are 100 and 152 pS, and expressed in BeWo cells, their conductance is 40, 116, and 189, all measured with CsCl as main pipette component [19]. In the same study, rat Cx40, expressed in Jeg-3 cells, had single channel conductances of 174 and 38 pS. When expressed in N2A, rat Cx40 conducted with 158 or 180 pS, with K-gluconate or KCl as main pipette component, respectively [17]. In half of the cell pairs also, smaller subconductance states equal to 21–48% of the main state were found. Finally, mouse Cx40 expressed in HeLa cells was reported to have single channel conductances of 121 and 153 pS with KCl as main pipette component [14], and newly formed mCx40 gap junction channels between HeLa cells showed one conductance of 198 pS and a residual conductance of 36 pS with K-aspartate as main pipette salt [18]. Therefore, when our experiments are compared with the data on hCx40, the data compare rather well, taking into account that CsCl conducts better than K-gluconate and results in 'larger' channels. However, rat or mouse Cx40 channels formed channels with substantially higher conductances than found in this study.

The smallest size found under control conditions was 30 pS. This conductance might either reflect the endogenously expressed Cx45 channel of SKHep1 cells, the conductance of which amounted 32–35 pS [33–35] or result from substates and residual conductances of Cx40 which were reported to amount within this 30 pS range [17,18].

After preincubation of the cells with cAMP, two conductances were found, i.e., 46 and 122 pS. The single channel conductance of ~80 pS observed under control conditions had disappeared after treatment with cAMP. Although in our experiments, where halothane is used to measure single channels, direct measurements of the open probability is not possible, some comparison between the histograms is valid, since they vary only by four events. The absence of the 80-pS conductance under cAMP conditions is not associated with a specific increased number of events in either the small or large conductance, indicating that this conductance has become inactive, rather than converted to the large or small conductance. While cAMP did not affect the largest conductance value, it increased the value of the smallest conductance from 30 to 46 pS. In previous experiments on identical cells, under highly similar conditions, Kwak et al. have shown that the single channel conductance is unaltered after exposure to cAMP [36]. This favours the option that this small conductance is Cx40 rather than Cx45 based. Since Cx40 and Cx45 are able to form heterotypical channels [37], the presence and modulation of Cx40/Cx45 heteromeric/heterotypical channels in these cells, cannot be excluded.

The shift in single channel conductances to larger values, as detected under halothane conditions might be partially responsible for the increase in macroscopic conductance (g_j) upon addition of cAMP. However, an indication for a more prominent role of increased open probability is seen in Fig. 4A and B. In both experiments, comparable concentrations of halothane were used to decrease P_o. When open, Cx40-channels under cAMP conditions seem to spend more time in this state than under control conditions (compare Fig. 4A and B).

4.4. Dye coupling

Preincubation of SKHep1/hCx40 cells with cAMP increased the amount of LY-stained cells by 58% as compared to control. Rat Cx40, transfected in N2A cells was shown to be cation selective, and the transfer of 2′,7′-dichlorofluorescein was not observed to increase with increasing junctional conductance [17]. However, no selectivity for anionic or cationic tracer molecules was observed for mouse Cx40, transfected in HeLa cells [37]. Although electrical conductance and permeability for dye tracers are not always parallely related [38], the increase of dye transfer was in our experiments accompanied by an increase in both single channel conductance and macroscopic conductance. The observed increase of LY-transfer by cAMP might either result from an increased permeability or result from an increased open probability of single channels, or a combination of these two effects. Since endogenous hCx45 channels in SKHep1 cells are impermeant for LY [35], interference of the endogenous channel is absent in these experiments.

4.5. Modulation of Cx40 in the heart

The increased conductance of Cx40 gap junctions by cAMP might also account for an electrical phenomenon found in the heart. When the rabbit heart is exposed to noradrenaline, thus raising intercellular cAMP levels [39], the conduction time decreases slightly in the atrium, strongly in the AV node but not in the His bundle [40]. Cx40 is found in the atrium, and all parts of the conduction system [2–6]. The effect of changes in intercellular coupling will, however, be most pronounced in regions were intercellular coupling is a limiting factor. Already in 1959, Hoffman et al. postulated that intercellular coupling presumably was one of the factors limiting the speed of action potential propagation within the AV node [41]. Indeed very scarce and small gap junctions composed of Cx40 and Connexin43 (Cx43) are found in the AV node [2,5]. Our experiments show that the macroscopic conductance of Cx40 gap junction channels is significantly increased by elevated cAMP levels. Although β-adrenergic stimulation increases the upstroke velocity of the AV nodal action potential, by upregulation of the L-type Ca-current [42–45], which leads to an improved action potential

conduction, an increased electrical conductance between AV nodal cells may also facilitate conduction of the action potential through the AV node in vivo.

In conclusion, we have shown that both microscopic and macroscopic electrical conductance, as well as the permeability for LY of gap junctions formed of Cx40 is increased by cAMP. In vivo, this may lead to an increase in intercellular conductivity and permeability in the vasculature and the heart where Cx40 is expressed.

Acknowledgements

The technical assistance of G.M. van Heeswijk is gratefully acknowledged. H.V.M.v.R. and A.A.B.v.V. are supported by the Netherlands Heart Foundation grant 97.184 (to H.J.J.). M.M.P.H. was supported by the Netherlands Organization for Scientific Research (NWO) grant 805–09.022 (to H.J.J.). We thank Dr. Ronald Wilders for critical reading of the manuscript and Dr. T.H. Steinberg for the anti-Cx45 antibody.

References

[1] Bruzzone R, White TW, Paul DL. Connections with connexins: the molecular basis of direct intercellular signaling. Eur J Biochem 1996;238:1–27.
[2] Gourdie RG, Severs NJ, Green CR et al. The spatial distribution and relative abundance of gap-junctional connexin40 and connexin43 correlate to functional properties of components of the cardiac atrioventricular conduction system. J Cell Sci 1993;105:985–991.
[3] Bastide B, Neyses L, Ganten D et al. Gap junction protein connexin40 is preferentially expressed in vascular endothelium and conductive bundles of rat myocardium and is increased under hypertensive conditions. Circ Res 1993;73:1138–1149.
[4] Gros D, Jarry-Guichard T, Ten Velde I et al. Restricted distribution of Connexin40, a gap junctional protein, in mammalian heart. Circ Res 1994;74:839–851.
[5] Davis LM, Kanter HL, Beyer EC, Saffitz JE. Distinct gap junction protein phenotypes in cardiac tissues with disparate conduction properties. J Am Coll Cardiol 1994;24:1124–1132.
[6] Van Kempen MJA, Ten Velde I, Wessels A et al. Differential connexin expression accommodates cardiac function in different species. Microscopy Res Techniq 1995;31:420–436.
[7] Verheule S, Van Kempen MJA, Te Welscher PHJA, Kwak BR, Jongsma HJ. Characterization of gap junction channels in adult rabbit atrial and ventricular myocardium. Circ Res 1997.
[8] Van der Velden HMW, Van Kempen MJA, Wijffels MCEF et al. Altered pattern of Connexin40 distribution in persistent atrial fibrillation in the goat. J Cardiovasc Electrophysiol 1998;9:596–607.
[9] Hennemann H, Suchyna T, Lichtenberg-Frate H et al. Molecular cloning and functional expression of mouse connexin40 a second gap junction gene preferentially expressed in lung. J Cell Biol 1992;117:1299–1310.
[10] Moore LK, Beyer EC, Burt JM. Characterization of gap junction channels in A7r5 vascular smooth muscle cells. Am J Physiol 1991;260:C975–C981.
[11] Beyer EC, Reed KE, Westphale EM, Kanter HL, Larson DM. Molecular cloning and expression of rat connexin40, a gap junction protein expressed in vascular smooth muscle. J Membrane Biol 1992;127:69–76.
[12] Little TL, Beyer EC, Duling BR. Connexin43 and Connexin40 gap junctional proteins are present in arteriolar smooth muscle and endothelium in vivo. Am J Physiol 1995;268:H729–H739.
[13] Bruzzone R, Haefliger JA, Gimlich RL, Paul DL. Connexin40, a component of gap junctions in vascular endothelium, is restricted in its ability to interact with other connexins. Mol Biol Cell 1993;4:7–20.
[14] Traub O, Eckert R, Lichtenberg-Fraté H et al. Immunochemical and electrophysiological characterization of murine connexin40 and −43 in mouse tissues and transfected human cells. Eur J Cell Biol 1994;64:101–112.
[15] Van Rijen HVM, Van Kempen MJA, Analbers US et al. Gap junctions in human umbilical cord endothelial cells contain multiple connexins. Am J Physiol 1997;272:C117–C130.
[16] Gabriels JE, Paul DL. Connexin43 is highly localized to sites of disturbed flow in rat aortic endothelium but Connexin37 and Connexin40 are more uniformly distributed. Circ Res 1998;83:636–643.
[17] Beblo DA, Wang HZ, Beyer EC, Westphale EM, Veenstra RD. Unique conductance, gating, and selective permeabilities properties of gap junction channels formed by Connexin40. Circ Res 1995;77:813–822.
[18] Bukauskas FF, Elfgang C, Willecke K, Weingart R. Biophysical properties of gap junction channels formed by mouse Connexin40 in induced pairs of transfected human HeLa cells. Biophys J 1995;68:2289–2298.
[19] Hellmann P, Winterhager E, Spray DC. Properties of Connexin40 gap junction channels endogeneously expressed and exogeneously overexpressed in human choriocarcinoma cell lines. Pflugers Archiv 1996;432:501–509.
[20] Kemp BE, Pearson RB. Protein kinase recognition sequence motifs. Trends Biochem Sci 1990;15:342–346.
[21] Kennely PJ, Krebs EG. Consensus sequences as substrate specificity determinants for protein kinases and protein phosphatases. J Biol Chem 1991;266:15555–15558.
[22] Kanter HL, Saffitz JE, Beyer EC. Molecular cloning of two cardiac gap junction proteins, Connexin40 and Connexin45. J Mol Cell Cardiol 1994;26:861–868.
[23] Hermans MMP, Kortekaas P, Jongsma HJ, Rook MB. pH sensitivity of the cardiac gap junction proteins, connexin45 and 43. Pflugers Arch 1995;431:138–140.
[24] Lowry OH, Rosebrough NJ, Farr AL, Randall RI. Protein measurement with the folin phenol reagent. J Biol Chem 1951;193:265–275.
[25] Laemmli UK. Cleavage of structural proteins during the assembly of the head of bacteriophage T4. Nature 1970;227:680–685.
[26] Schoenmakers TJM, Visser GJ, Flik G, Theuvenet APR. CHELATOR: An improved method for computing metal ion concentrations in physiological solutions. BioTechniques 1992;12:870–879.
[27] Neyton J, Trautmann A. Single-channel currents of an intercellular junction. Nature 1985;317:331–335.
[28] White RL, Spray DC, Campos de Carvalho AC, Wittenberg BA, Bennett MVL. Some electrical and pharmacological properties of gap junctions between adult ventricular myocytes. Am J Physiol 1985;249:C447–C455.
[29] Johnston MF, Simon SA, Ramón F. Interaction of anaesthetics with electrical synapses. Nature 1980;286:498–500.
[30] Burt JM, Spray DC. Volatile anaestetics block intercellular communication between neonatal rat myocardial cells. Circ Res 1989;65:829–837.
[31] Van Rijen HVM, Wilders R, Van Ginneken ACG, Jongsma HJ. Quantitative analysis of dual whole-cell voltage–clamp determination of gap junctional conductance. Pflugers Arch 1998;436:141–151.
[32] Stewart WW. Lucifer dyes, highly fluorescent dyes for biological tracing. Nature 1981;292:17–21.
[33] Laing JG, Westphale EM, Engelmann GL, Beyer EC. Characteriza-

tion of the gap junction protein, Connexin45. J Membr Biol 1994;139:31–40.
[34] Moreno AP, Laing JG, Beyer EC, Spray DC. Properties of gap junction channels formed of connexin45 endogenously expressed in human hepatoma (SKHep 1) cells. Am J Physiol 1995;268:C356–C365.
[35] Kwak BR, Hermans MMP, De Jonge HR et al. Differential regulation of distinct types of gap junction channels by similar phosphorylating conditions. Mol Biol Cell 1995;6:1707–1719.
[36] Kwak BR, Jongsma HJ. Regulation of cardiac gap junction channel permeability and conductance by several phosphorylating conditions. Mol Cell Biochem 1996;157:93–99.
[37] Elfgang C, Eckert R, Lichtenberg-Frate H et al. Specific permeability and selective formation of gap junction channels in connexin-transfected HeLa cells. J Cell Biol 1995;129:805–817.
[38] Kwak BR, Van Veen TAB, Analbers US, Jongsma HJ. TPA increases conductance but decreases permeability in neonatal rat cardiomyocyte gap junction channels. Exp Cell Res 1995;220:456–463.
[39] Sugiyama A, McKnite S, Wiegn P, Lurie KG. Measurement of cAMP in the cardiac conduction system of rats. J Histochem Cytochem 1995;43:601–605.
[40] Antoni H. Function of the heart. In: Schmidt RF, Thews G, editors, Human physiology, 2nd ed, Berlin Heidelberg: Springer-Verlag, 1989, pp. 439–479.
[41] Hoffman BF, Paes de Carvalho A, Mello WC, Cranefield PF. Electrical activity of single fibers in the atrioventricular node. Circ Res 1959;7:11–18.
[42] Reuter H, Scholz H. The regulation of the calcium conductance of cardiac muscle by adrenaline. J Physiol 1977;264:49–62.
[43] Noma A, Irisawa H, Kokobun S et al. Slow current systems in the A-V node of the rabbit heart. Nature 1980;285:228–229.
[44] Brum G, Osterrieder W, Trautwein W. β-Adrenergic increase in the calcium conductance of cardiac myocytes studied with the patch clamp. Pflugers Arch 1984;401:111–118.
[45] Han X, Kobzik L, Balligand JL, Kelly RA, Smith TW. Nitric oxide synthase (NOS3)-mediated cholinergic modulation of Ca^{2+} current in adult rabbit atrioventricular nodal cells. Circ Res 1996;78:998–1008.